Solution Conformation of the Met 61 to His 61 Mutant of *Pseudomonas stutzeri* ZoBell Ferrocytochrome c-551

Gregory T. Miller,* John K. Hardman,† and Russell Timkovich*
Departments of *Chemistry and †Biology, University of Alabama, Tuscaloosa, Alabama 35487 USA

ABSTRACT The gene encoding for bacterial cytochrome c-551 from *Pseudomonas stutzeri* substrain ZoBell has been mutated to convert the invariant sixth ligand methionine residue into histidine, creating the site-specific mutant M61H. Proton NMR resonance assignments were made for all main-chain and most-side chain protons in the diamagnetic, reduced form at pH 9.2 and 333 K by two-dimensional NMR techniques. Distance constraints (1074) were determined from nuclear Overhauser enhancements and main-chain torsion-angle constraints (72) from scalar coupling estimates. Solution conformations for the protein were computed by the simulated annealing approach. For 28 computed structures, the root mean squared displacement from the average structure excluding the terminal residues 1, 2, 81, and 82 was 0.52 Å ($\sigma = 0.096$) for backbone atoms and 0.90 Å ($\sigma = 0.122$) for all heavy atoms. The global folding of the mutant protein is the same as for wild type. The biggest changes are localized in a peptide span over residues 60–65. The most striking behavior of the mutant protein is that at room temperature and neutral pH it exists in a state similar to the molten globular state that has been described for several proteins under mild denaturing conditions, but the mutant converts to a more ordered state at high pH and temperature.

INTRODUCTION

Cytochromes of the c-type have a heme prosthetic group covalently attached to peptide by thioether bonds and normally have histidine and methionine as ligands to the iron. Cytochromes of the b-type have noncovalently associated heme and usually, but not exclusively, His-His ligation. The gene *nir M* encoding cytochrome c-551 in *Pseudomonas stutzeri* substrain ZoBell was engineered to change the normal methionine heme ligand (Met 61) to a histidine, thereby converting a normal c-type cytochrome into a hybrid b/c-type. Mutant protein M61H was expressed in *Escherichia coli*, purified, and characterized in terms of its unusual biochemical properties (Miller et al., 2000). The solution structure of M61H has now been determined by NMR and is reported herein. Some degree of structural change in the protein was anticipated, because Met 61 performs an essential role and has been found to be an invariant ligand in all known members of the bacterial c-551 family and the mitochondrial cyt c family. The unexpected result was that this apparently simple single-site change dramatically affected the dynamics of the protein and converted a very rigid molecule into a room-temperature, neutral pH, molten-globule-like state.

MATERIALS AND METHODS

Mutant protein was prepared and purified as described previously (Miller et al., 2000). NMR spectra were recorded at 500 MHz and processed with FELIX software. Sample preparation and spectroscopic details for the collection of HOHAHA, NOESY, and DQF-COSY spectra were as described previously (Timkovich et al., 1998). Macromolecular structure calculations were performed with the software suite CNSsolve, version 0.9a (Brunger et al., 1998), and different protocols for use will be discussed under Results.

RESULTS AND DISCUSSION

Cytochromes c-551 characteristically give well behaved protein NMR spectra. In the reduced state the iron is low-spin ferrous, and hence the ferrocytochrome is diamagnetic without paramagnetic line broadening. It is a compact globular protein giving rise to relatively narrow line-shapes due to its fast rotational correlation time, and resonances are well dispersed because of the strong ring current of the heme (see Fig. 1 *D*). Previous solution structures (Cai et al., 1992; Cai and Timkovich, 1994, 1999; Chau et al., 1990; Timkovich et al., 1998) were based upon spectra taken at slightly acidic pH values, in principle, to slow down exchange of main-chain amides. In practice, main-chain amides exchanged slowly at all pH values with one exception, Gln58 in *Nitrosomonas* c-552 (Timkovich et al., 1998), and useful data have been recorded from pH 2 to 12 (Cai and Timkovich, 1992), often allowing ambiguous assignments to be clarified because of selective pH-linked chemical shift changes (Cai and Timkovich, 1991). The ferrocytochrome M61H surprisingly did not follow this pattern. Fig. 1 *A* displays the NMR spectrum of M61H at room temperature and pH 4.7. The mutant protein precipitates at pH values below 4.3, whereas the wild-type protein is soluble to pH 3.8. Fig. 1 *B* is the spectrum at room temperature and pH 7.0. Compared with the spectrum of the wild-type c-551 (Fig. 1 *D*), one sees broad lines for most of the resolved resonances above 9 ppm, a lack of dispersion of resonances, and a broad envelope between 7 and 9 ppm. The

Received for publication 15 November 2000 and in final form 5 March 2001.

Address reprint requests to Dr. Russell Timkovich, Department of Chemistry, PO Box 870336, University of Alabama, Tuscaloosa, AL 35487-0336. Tel.: 205-348-8439; Fax: 205-348-9104; E-mail: rtimkovi@bama.ua.edu.

0006-3495/01/06/2928/07 $2.00

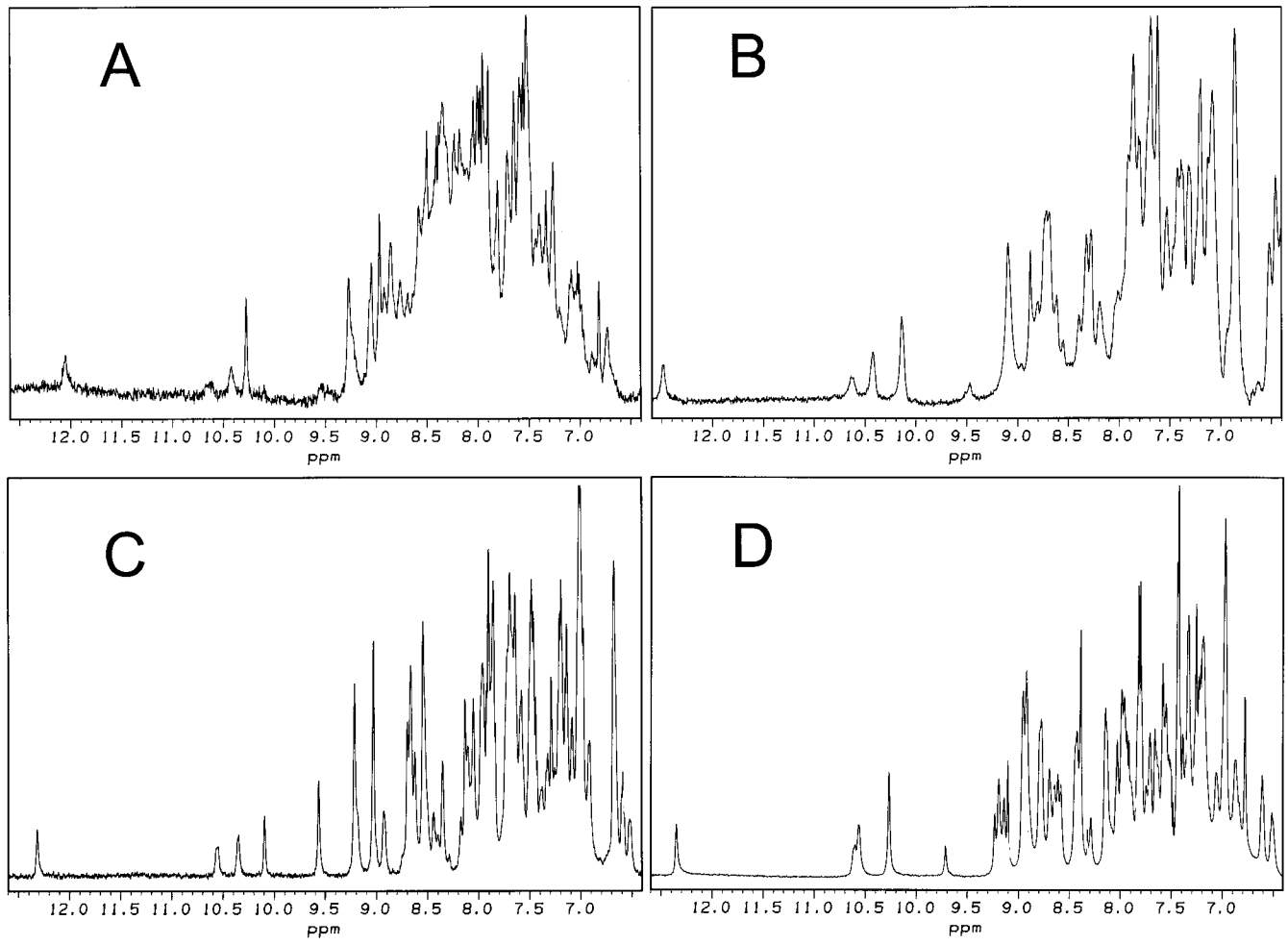

FIGURE 1 ^{1}H-NMR spectra of the aromatic region of mutant and wild-type ferrocytochrome c-551 in 90% protic buffer. (*A*) M61H at pH 4.7 and 296 K; (*B*) M61H at pH 7.0 and 296 K; (*C*) M61H at pH 9.2 and 333 K; (*D*) Wild-type c-551 at pH 7.0 and 296 K.

features at pH 4.7 or 7.0 did not change substantially when samples were heated or cooled. The spectrum at pH 4.7 does show some sharp features in the broad envelope.

The protein samples were highly purified as shown by high-pressure liquid chromatography and silver-staining of SDS-polyacrylamide gel electrophoresis gels (see Miller et al., 2000). Protein aggregation could contribute to poor spectral quality. However, the mutant protein behaved identically to wild type in size-exclusion chromatography and during gel electrophoresis under non-denaturing conditions. NMR spectra were not concentration dependent over the range 0.2–5.0 mM. Optical adsorption spectra of the mutant confirmed that the reduced form was low spin, $S = 0$. Ferrocytochromes c-551 are subject to severe line broadening in the presence of traces of ferricytochrome because their high electron self-exchange rate leads to chemical exchange between a diamagnetic and a paramagnetic form (Timkovich et al., 1988). All reduced mutant samples were prepared in deoxygenated buffer by reduction with excess dithionite under an inert atmosphere and sealed in NMR tubes under argon. Raising the pH of the sample to 9.2 and increasing the temperature to 323–343 K did convert the spectrum into one more typical of a c-551 (Fig. 1 *C*). Raising the pH alone improved the spectrum, but the temperature increase was also needed to achieve the line-widths of wild-type samples at room temperature.

The spectra of M61H compared with wild type are very similar to what was observed when horse cyt c was converted to a non-compact molten-globular-like state at pD 2.2 in 0.1 M NaCl (see especially Fig. 1 of Jeng and Englander, 1991). The M61H spectrum at pH 4.7 is similar to Fig. 1E of Jeng and Englander (1991), and the sharp features imposed on the broad envelope may represent portions of the molecule that are close to random coil. M61H at pH 7.0 is more similar to their Fig. 1C, where there is less random coil and more molten globule. Jeng and Englander have pointed out that the term molten globule is imprecisely defined, but it does convey some liquid-like character and disorder with respect to the more compact and stable native state. Side chains and segments of main chain

may be disordered while a relatively compact overall conformation and considerable secondary structure is retained. This state has been observed for several globular proteins but normally requires high temperature, extremes of pH or ionic strength, and/or the presence of a chemical denaturant. The mutant is a bizarre example whereby the NMR spectrum is molten-globule-like at room temperature and neutral pH but becomes native-like at elevated pH and high temperature.

Qualitative studies on hydrogen-deuterium exchange also indicated that M61H at neutral pH had a loose conformation. Samples of mutant and wild-type protein were dialyzed against protic 50 mM ammonium bicarbonate and lyophilized. They were then dissolved in 50 mM phosphate buffer in 99.8% ^2H_2O, pD 7.0, deoxygenated by cycles of argon flushing and vacuum, reduced with dithionite, and sealed in NMR tubes under argon. The time to complete these operations and record a one-dimensional NMR spectrum at 296 K was ~45 min. Fig. 2 *A* shows the specrum of wild-type protein after 45 min of deuterium exchange. Multiple NH resonances are still present because of the slow rate of exchange. Previous studies on c-551 have shown that 36 of the 82 amides have half-times for exchange in excess of 300 min (Timkovich et al., 1992). Fig. 2 *B* shows M61H after the same period of exchange, and it is evident that far more amides have exchanged.

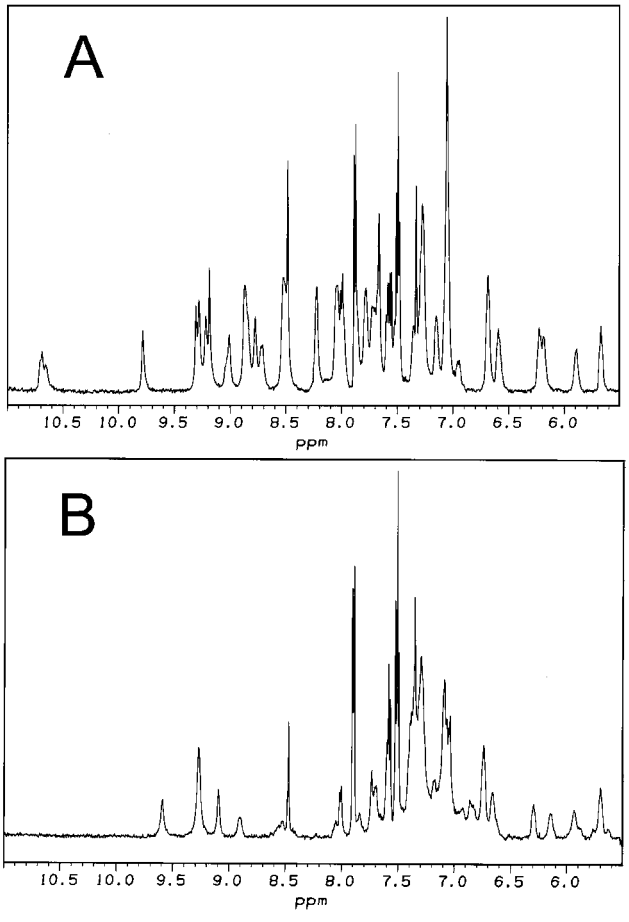

FIGURE 2 ^{1}H-NMR spectra of the aromatic region of mutant and wild-type ferrocytochrome c-551 in 99.8% deuterated buffer at room temperature and neutral pH after 45 min of exchange from the lyophilized protic state. (*A*) Wild-type protein; (*B*) M61H mutant.

In hemoproteins, only the deprotonated imidazole ring has an electron lone pair that can coordinate to iron. Because the new ligand in the mutant is histidine, an obvious hypothesis is that the transition at elevated pH is linked to deprotonation of an imidazolium ring of His61 not bonded to Fe at neutral pH, followed by binding at high pH. There are several pieces of evidence against this. Optical spectroscopy has shown that the visible spectrum of M61H is typical of a low-spin coordination sphere with two strong field ligands over a wide range of pH and temperature. In general, when heme becomes penta-coordinated, or a strong field ligand is replaced by a weak field one, the visible spectrum changes to a globin-like high-spin form. In mitochondrial cytochromes c, the methionine ligand can be replaced under certain circumstances by a lysine side chain, in what is known as the alkaline transition, and the visible spectrum stays low spin (Kaminsky et al., 1973). However, in c-551 there are no lysyl residues close enough to the heme to perform this function, and wild-type c-551 does not undergo this type of transition. In NMR assignments at pH 9.2 to be subsequently discussed, a Cβ proton of His 61 was found at −1.2 ppm. The unusual shift is due to the heme ring current, which rapidly changes away from the heme. This resonance is resolved and readily observed in one-dimensional NMR spectra. It was observed at pH 4.7 and 7.0 at all temperatures, albeit broadened at pH values below 9.2 (−1.27 ppm and 40 Hz at pH 4.7; −1.24 ppm and 20 Hz at pH 9.2)

NOESY and HOHAHA spectra of M61H at pH 7.0 gave very few cross-peaks, presumably due to rapid relaxation during the mixing time and chemical exchange among multiple (disordered) conformations. No assignments were possible except for a few by homology associated with resolved resonances in one-dimensional spectra. Therefore, no precise information could be obtained for the site or sites of disorder. Two-dimensional spectra at pH 9.2 and 323–343 K did yield interpretable cross-peaks, although it should be added that the quality of the spectra were not as high as for wild-type c-551s, and certain assignment problems arose that will be discussed.

Sequential assignments were made as for previous c-551s and have been deposited in the BioMagResBank as entry BMRB-4960. Shifts in the mutant were highly homologous to wild type. This is illustrated in Fig. 3, which compares main-chain amide and CαH chemical shifts. The biggest differences are in the span 58–64, which in wild type forms a polyproline-type helix that orients the 61 ligand for coordination to iron. A major assignment problem was that 10 expected main-chain amide resonances did not appear in

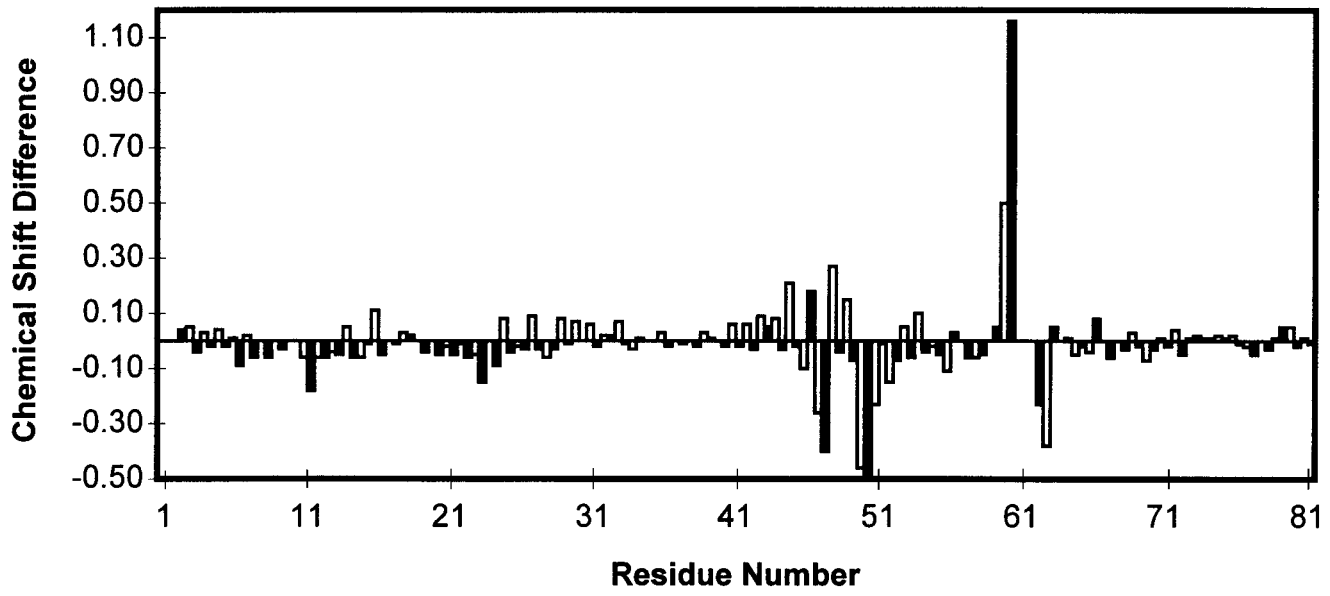

FIGURE 3 Chemical shift differences between M61H and wild-type resonances. The open bars represent main-chain amide resonances, and the solid bars represent CαH resonances.

NOESY or HOHAHA spectra of the fingerprint region. These were for D2, G3, V18, K21, G36, E38, G39, A41, E68, and E69. They are in fast exchange with the water solvent. This would be a major problem in a de novo protein structure determination by NMR because of the serious breaks in sequential connectivity. For the mutant so homologous to wild type, it was still possible to assign CαH and side-chain protons for these residues based upon scalar coupling and inter-residue NOEs for the non-exchangeable protons.

Scalar coupling of the spin system of His 61 was evident in HOHAHA and DQF-COSY spectra. Sequential connectivity was established by NOEs from the amide to Pro60 CαH and CβH. In the global folding of wild-type c-551s, conserved residues Gly 51 and Ser 52 are close in space to residue 61. Accordingly, critical NOEs were observed for 61 NH $\leftrightarrow$ {52 NH, 52 CβH}, for 61CβHs $\leftrightarrow$ {52 CαH, 52CβHs, and 51CαH}; 61 NH and 61 CβH also gave clear NOEs to the heme propionate 13^2 protons. NOEs from 61CβHs to 61 HD1 (Protein Data Bank nomenclature, also denoted Nδ_1H or NπH in IUPAC-IUB nomenclature) were critical in assigning the imidazole protons. 61 HD1 gave strong NOE and HOHAHA cross-peaks to 61 HE1 (Cϵ_1H), enabling its firm assignment. Additional confirming NOEs were observed between the 61 ring protons and Asn 64 side-chain amide protons, Ile 48 CαH and 48 CγHs, and Pro 62 CγHs.

To the best of the authors' knowledge, when histidine ligates to heme it is invariably through the lone electron pair on Nϵ_2 (also denoted Nτ) of the imidazole ring. This appears to also be the case for M61H. Unfortunately, we were unable to obtain a firm assignment for His 61 HD2 (Cδ_2H); but, only strong scalar connectivity was observed between HD1 and HE1, consistent with an Fe-Nϵ_2 bond. If the bond were Fe-Nδ_1, then strong coupling should have been observed for Cϵ_1H to Nϵ_2H and Nϵ_2H to Cδ_2H.

Upon comparing the chemical shifts of ring protons of His 61 with the other heme ligand His 16, the HD1 protons are found to be similar, 9.2 for H61 versus 8.5 ppm for H16. These values are similar to normal histidine residues in spite of the close proximity of the heme plane ring current, because the protons are situated close to the nodal cone where the ring current effect changes from shielding to deshielding. The HE1 protons are very different, 4.16 ppm for H61 versus 0.69 ppm for H16, but both are shifted to low frequency by the heme ring current. A survey of the Protein Data Bank of NMR-determined structures revealed that cytochrome b5 was the only bis-histidine hemoprotein deposited with assigned ligand ring protons (Guiles et al., 1992). Only the ring protons of the heme ligand His 63 were reported, 0.76 ppm for HE1 and 0.23 ppm for HD2, similar to the values for His 16 in the present case (0.69 and 0.58 ppm). Why is His 61 in M61H different? It is highly unlikely that there is any significant distortion of the 61 ligand geometry compared with 16. It is more reasonable that the heme ring current is not symmetrical across or along the ring. We have used simple symmetrical ring current models (Shulman et al., 1970) to calculate ring current shifts for protons close to the heme in wild-type c-551. Agreement can be obtained for some but not all of the observed chemical shifts, which suggests there is asymmetry.

NOE distance constraints (1039) and main-chain dihedral angle constraints (72) were estimated from NOESY and HOHAHA spectra as described previously (Timkovich et

al., 1998). Values in this set of constraints were very similar to those observed in determining the solution conformation of the wild-type protein (Cai and Timkovich, 1994), with the obvious exceptions of new constraints for the mutated side chain and some changes in neighboring residues. The level of expression of the mutant protein is not high enough to allow preparation of isotopically enriched samples at feasible costs, so the set of constraints is limited to what can be obtained on natural abundance samples. Calculation of the solution conformation of M61H began by replacing the atomic coordinates of the Met 61 residue in the Protein Data Bank file 1CCH for wild-type *Pseudomonas* ZoBell c-551 with an idealized histidyl side chain. This was done using the Biopolymer module of the macromolecular modeling software package SYBYL (Tripos Associates, St. Louis, MO). The substitution is "dumb" in that the resultant imidazole ring is not properly oriented as an iron ligand and has severe van der Waals violations with other nearby atoms. This distorted geometry molecule was used as a template file for a first series of computations.

Initial simulated annealing calculations were performed using a protocol described previously (Timkovich et al., 1998) or by a standard protocol (anneal.inp) distributed with CNSsolve (Brunger, 2000) employing the second Cartesian slow cooling option. The results were similar, and the standard CNSsolve protocol was subsequently used exclusively. Thirty-five hydrogen bonds in the four main helical segments of c-551 were identified from the initial calculations and were included as pseudo-NOE constraints as described previously (Timkovich et al., 1998). Thirty-five simulated annealing structures were computed with the expanded constraint set. Of these, 28 had no NOE violations greater than 0.5 Å, and 7 each had one random violation greater than 0.5 Å. The average over the 35 structures of the root mean squared NOE violation was 0.040 Å. There were no torsion-angle violations greater than 5°, and the average root mean squared violation was 0.051°. The 28 structures with no NOE violations greater than 0.5 Å were averaged and energy minimized to compute the final structure for M61H. The root mean squared displacement (RMSD) from the average structure excluding the terminal residues 1, 2, 81, and 82 was 0.52 Å ($\sigma = 0.096$) for backbone atoms and 0.90 ($\sigma = 0.122$) for all heavy atoms. The energy-minimized structure had no torsion-angle violations greater than 5°, 24 NOE violations greater than 0.1 Å, 4 NOE violations greater than 0.25 Å, and no NOE violations greater than 0.5 Å. The RMSDs were as follows: for NOE violations, 0.038 Å; for torsion violations, 0.052°; for bonds, 0.0046 Å; for angles, 0.88°; and for improper angles, 0.77°. The total NOE energy term was 119 kcal based upon the standard CNSsolve NOE energy scale of 75 kcal.

The above structure calculation is subject to the criticism that it started from basically the wild-type global fold. In part this may be justified by the close correspondence of chemical shifts between mutant and wild-type protein (Fig. 3), but it was straightforward to show that the final result was not prejudiced by this choice. A standard CNSsolve utility (generate_extended.inp) was used to generate a random coil version of the mutant with correct local geometry. This was then used as the starting template for distance geometry calculations with substructure embedding. The embedded structures were then regularized by the same CNS simulated annealing protocol described above. Thirty distance geometry-simulated annealing (DGSA) structures were calculated. Of these, 26 had no NOE violations greater than 0.5 Å, 2 had one random violation, and 2 had two random violations. The average over the 30 DGSA structures of the root mean squared NOE violation was 0.042 Å. There were no torsion violations greater than 5°, and the average root mean squared violation was 0.058°. The DGSA structures showed the same hydrogen bonds that were identified in the first series of calculations. This is not surprising because these hydrogen bonds are distributed among the four major sections of α-helix in the molecule, and these sections are already implicated as helical by their torsion angles and the characteristic sequential NOEs associated with helical secondary structure. All 30 DGSA structures were averaged and energy minimized. For this average structure, RMSDs were as follows: for NOE violations, 0.035 Å; for torsion violations, 0.099°; for bonds, 0.0044 Å; for angles, 0.86°; for improper angles, 0.72°; and the total NOE energy term was 101 kcal. Most importantly, the RMSD of the atoms of this average DGSA structure compared with the average structure computed starting from the folded template was 0.47 Å for backbone atoms and 0.75 Å for all heavy atoms. The minimized, average solution structure for M61H has been deposited with the RCSB Protein Data Bank as entry 1FI3.

The mutant structure retains the global folding and critical features found in wild type. The hydrogen-bonding network around the heme propionates is intact. This network has been implicated in modulating the redox potential of the heme with respect to pH (Cai and Timkovich, 1992). In the mutant, the redox potential at pH 7 is 200 mV lower than in wild type, but the redox potential still retains its characteristic dependence upon pH (Miller et al., 2000).

In the simulated annealing calculations, the heme-histidine bonds (Fe-Nϵ_2) were given an equilibrium value taken from the x-ray crystal structure of *P. aeruginosa* c-551 (Matsuura et al., 1982), but that bond was also constrained to be normal to the heme plane by improper torsion angles. We know of no crystal structure of a hemoprotein or model compound where this type of bond would be significantly bent from the ring normal, and it is doubtful that the current constraint set data would detect such an eventuality anyway. However, no improper constraints were placed on the orientation of the imidazole plane about the Fe-Nϵ_2 axis. Fig. 4 is a stereodiagram of the first 10 of the 28 accepted simulated annealing structures showing the heme ring and the imidazole rings of His 61 and His 16. The latter rings

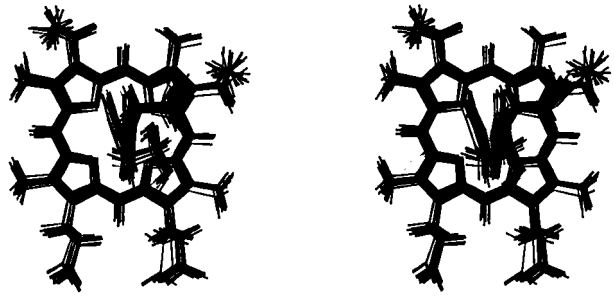

FIGURE 4 Stereodiagram of the superimposition of the first 10 simulated annealing structures of M61H showing the relation of the two histidine ligands to the heme.

have a well defined orientation determined by the experimental constraints and the standard peptide geometry. Multiple NOEs exist between imidazole protons, heme protons, and protons of neighboring side chains in the heme crevice. The plane angle between the imidazoles averages to 22°.

The largest differences between M61H and wild-type structures were in the peptide span 60–65, illustrated in the stereodiagram of Fig. 5. In particular, the ring of His 61 does not allow the side chain of Asn 64 to pack against the heme in the normal way, due to steric hindrance with His HD1 and HE1. The proline rings of P62, 63, and especially 65 are displaced from their wild-type orientation. Fig. 3 also indicates that some of the largest relative changes in chemical shift appear for residues in the 45–52 span, but even these are at most 0.5 ppm. No significant structure rearrangement was evident in the calculated M61H conformation compared with the RMSDs of the ensemble. The 45–52 span in question is at the end of the 40's main helix and butts up against the polyproline-type helix that orients H61 for ligation. In fact, in both wild type and M61H there are significant NOEs between 52NH and 61NH (very strong) and between 61NH and the side-chain protons of S52 and G51. It may be that the chemical shift differences reflect a through-space environment change rather than a structural perturbation.

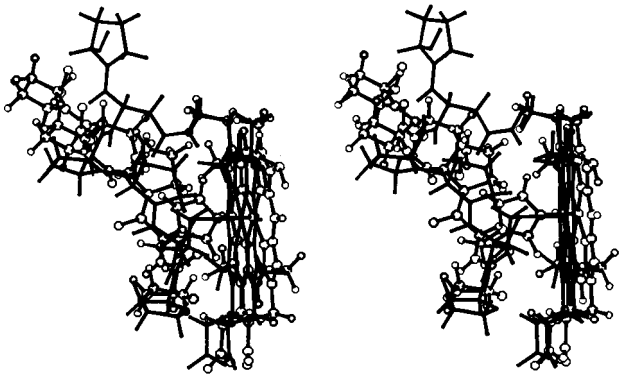

FIGURE 5 Stereodiagram comparing the peptide structure in the span 60–65 of M61H (ball and stick figure) with wild type (stick only figure).

Structural changes are minimal and corroborate the similarities observed in some of the physiochemical properties between the two proteins (Miller et al., 2000). The mutant is similar in temperature stability toward conversion to a high-spin form. It is slightly more susceptible to complete denaturation by guanidinium hydrochloride or low pH but is still remarkably stable compared with other proteins. The mutant had an apparent maximal velocity 2.7-fold less as an electron donor to the *Pseudomonas* nitrite reductase, but the apparent Michaelis-Menten constant was also 3.4-fold less, suggesting tighter binding of the mutant to the nitrite reductase. The most obvious change in the mutant was a decrease by ~200 mV in its reduction potential. The solution conformation of M61H implicates the loss of sulfur ligation as the major factor in this change. The minor rearrangement of residues packing against the heme may contribute in some degree to the redox change but is unlikely to be the dominant factor. A major rearrangement could have been more of a contributor, such as if the peptide span had opened to allow solvent exposure to the otherwise buried heme.

The similarity of M61H at pH 9.2 and 333 K to wild type does not explain the molten-globular-like NMR spectra of the mutant under more physiological conditions. Loss of His 61 ligation has been ruled out as the cause, based upon the low-spin visible spectrum and the His 61 CβH marker resonance. The only other obvious ionizable group whose change might be expected to disrupt structure, especially near the heme, is the ring of His 47, which is involved in hydrogen bonding to the heme-buried propionate. This histidine has been shown to have a pK_a of 8.2 in *P. stutzeri* ferrocytochrome c-551 (Cai and Timkovich, 1992). However, its protonation-deprotonation had minimal impact on the wild-type structure. The ionization state of His 47 in the mutant cannot be followed, because of the poor quality of the two-dimensional spectra below pH 9.2. It may be that there is an unexpected synergistic effect if His 61 is present. Alternatively, there may not be a single ionization site causing the transformation. It may be due to cumulative, broad effects involving both pH and temperature. His 61 and the peptide span 60–65 refined to well defined conformations in the final structure. At normal temperature and pH they may be disordered without breaking the His-Fe bond, such as a scenario involving rotations about the Fe-Nϵ_2 bond, which could transmit disruptions to other segments. This is a fascinating and totally unexpected situation to accompany what otherwise seems to be an innocuous mutation.

This work was supported in part by grant GM59035 (R.T.) from the National Institutes of Health.

REFERENCES

Brunger, A. T. 2000. Crystallography and NMR System. http://xplor.csb.yale.edu/cns_solve.

Brunger, A. T., P. D. Adams, G. M. Clore, W. L. DeLano, P. Gros, R. W. Grosse-Kunstleve, J.-S. Jiang, J. Kuszewski, M. Nilges, N. S. Pannu, R. J. Read, L. M. Rice, T. Simonson, and G. L. Warren. 1998. Crystallography and NMR system: a new software suite for macromolecular structure determination. *Acta Crystallogr.* D54:905–921.

Cai, M., E. G. Bradford, and R. Timkovich. 1992. Investigation of the solution conformation of cytochrome c-551 from *Pseudomonas stutzeri*. *Biochemistry.* 31:8603–8612.

Cai, M., and R. Timkovich. 1991. Proton resonance assignments for *Pseudomonas aeruginosa* ferrocytochrome c-551. *Biochem. Biopyhs. Res. Commun.* 178:309–314.

Cai, M., and R. Timkovich. 1992. Ionization of the heme porpionate substituents in pseudomonad cytochromes c-551. *FEBS Lett.* 311: 213–216.

Cai, M., and R. Timkovich. 1994. The solution conformation of cytochrome c-551 from *P. stutzeri ZoBell* determined by NMR. *Biophys. J.* 67:1207–1215.

Cai, M., and R. Timkovich. 1999. Solution conformation of ferricytochrome c-551 from *Pseudomonas stutzeri* substrain ZoBell. *Biochem. Biophys. Res. Commun.* 254:675–678.

Chau, M. H., M. Cai, and R. Timkovich. 1990. NMR comparison of prokaryotic and eukaryotic cytochromes c. *Biochemistry*. 29: 5076–5087.

Guiles, R. D., V. J. Basus, I. D. Kuntz, and L. Waskell. 1992. Sequence specific ^{1}H and ^{15}N resonance assignments for both equilibrium forms of the soluble heme binding domain of rat ferrocytochrome b_5. *Biochemistry.* 31:11365–11375.

Jeng, M.-F., and S. W. Englander. 1991. Stable submolecular folding units in a non-compact form of cytochrome c. *J. Mol. Biol.* 221:1045–1061.

Kaminsky, L. S., V. J. Miller, and A. J. Davison. 1973. Thermodynamic studies of the opening of the heme crevice of ferricytochrome c. *Biochemistry.* 12:2215–2221.

Matsuura, Y., T. Takano, and R. E. Dickerson. 1982. Structure of cytochrome c551 from *P. aeruginosa* refined at 1.6 Å resolution, and comparison of the two redox forms. *J. Mol. Biol.* 156:389–409.

Miller, G. T., B. Zhang, J. K. Hardman, and R. Timkovich. 2000. Converting a c-type to a b-type cytochrome: Met61 to His 61 mutant of *Pseudomonas* cytochrome c-551. *Biochemistry.* 39:9010–9017.

Shulman, R. G., K. Wuthrich, T. Yamane, D. J. Patel, and W. E. Blumberg. 1970. Nuclear magnetic resonance determination of ligand-induced conformational changes in myoglobin. *J. Mol. Biol.* 53:143–157.

Timkovich, R., D. Bergmann, D. M. Arciero, and A. B. Hooper. 1998. Primary sequence and solution structure for ferrocytochrome c-552 from *Nitrosomonas europaea*. *Biophys. J.* 75:1964–1972.

Timkovich, R., M. Cai, and D. W. Dixon. 1988. Electron self-exchange in *Pseudomonas* cytochromes. *Biochem. Biophys. Res. Commun.* 150: 1044–1050.

Timkovich, R., L. A. Walker II, and M. Cai. 1992. Hydrogen exchange in *Pseudomonas* cytochrome c-551. *Biochim. Biophys. Acta.* 1121:8–15.